Colin Murphy

Chem 3397, Spring 2015

Section 2

Fuel Cell

Full Format #1

Group # 3

Date Started: 2-18-15

Date Completed: 2-18-15

Date Submitted: 4-20-15

Abstract

Using a small and simple thin-layer fuel cell deign, the performance of two unitized regenerative fuel cells was studied. The substantial power obtained from these small fuel cells, which require a small amount of electrolyte and pose very little danger, provides high-energy density with minimized surface area. The cells utilized two different aqueous electrolyte solutions: NaCl (0.3327 ± .0003 M), operating as a hydrogen-chlorine fuel cell; Na_2SO_4 (0.06689 ± .00007 M), operating as a hydrogen-oxygen fuel cell. The performance of each cell was studied by applying 2 sets of external resistors (909-200 kΩ and 150-10 kΩ) in decreasing then increasing order. The hydrogen-chlorine fuel cell showed very little hysteresis, while the hydrogen-oxygen cell exhibited a much lower power density and greater loss of power. The H_2/Cl_2 cell provided a maximum power of ~7.28 W m^{-2}, while the H_2/O_2 cell was only capable of a 0.81 W m^{-2} maximum power. The fuel cells were also studied as realistic energy sources to power a calculator and LED light. Both cells provided steady power for the calculator, but both cells exhibited an exponential decay in current when powering the LED, with H_2/Cl_2 providing power for ~5 minutes and H_2/O_2 for ~1 minute. The performance of the hydrogen-chlorine fuel cell, having provided reproducible and long lasting power (relative to its size), was found to be much greater than that of the hydrogen-oxygen cell.

Introduction

Fuel cells generate electricity from the chemical energy produced by a redox reaction. The redox reaction consists of two half reactions, oxidation and reduction, which occur at the anode and cathode respectively. In the pursuit of environmentally friendly fuel sources, to replace those of fossil fuels, significant research has been applied to developing and improving fuel cells [1].

The predicted voltage produced by a fuel cell is given by the Nernst equation, represented in equation 1:

$$E_{cell} = E^{\circ}_{cell} - \frac{RT}{nF}\ln(Q) \qquad (1)$$

where E°_{cell} is the standard cell potential, *R* is the molar gas constant, *T* is temperature, *n* is the number of electrons involved in the redox reaction, *F* is Faraday's constant, and *Q* is the reaction quotient. Under standard conditions (1 M of reactants, 25° C, and 100 kPa), the reaction quotient would be 1, resulting in ln(1) to be zero; thus, the potential of the cell will depend only on the standard cell potential. This standard cell potential is derived from the standard reduction and oxidation potentials of the two redox half reactions. The equation used to determine the standard cell potential represented in equation 2:

$$E^{\circ}_{cell} = \text{oxidation potential} + \text{reduction potential} \qquad (2)$$

where the oxidation potential and reduction potentials are standard potentials given in tables [2].

The redox reaction occurring within a fuel cell is an example of a spontaneous chemical reaction and is limited by the amount of fuel; this cell is therefore considered a galvanic cell and its cell potential will be positive. The other type of electrochemical cell is called an electrolytic cell, which uses an external power source to drive a non-spontaneous electrochemical decomposition, resulting in a negative cell potential. One type of fuel cell, known as a regenerative fuel cell, can be recharged by reproducing reactants through a separate electrolyzer unit, storing the reactants and then reused to produce electricity. The combination of these two capabilities into a single cell, so that the cell may function as either an electrolyzer or a fuel cell, is known as a unitized regenerative fuel cell (URFC).

In order to access reactants required when operating as an electrolyzer or fuel cell, a specific design is required for the URFC to easily switch between the two operating modes. By applying an external power source, such as solar cell, the unit operates in electrolyzing mode, producing gasses (e.g. hydrogen and chlorine or hydrogen and oxygen) at the respective electrodes. When the external power source is removed, the unit operates as a fuel cell.

In this experiment, two different thin-layer URFCs were characterized as electrolyzers and fuel cells. Their performance as regenerative fuel cells were also studied and compared. Both cells utilized the same cell design, but differed in fuel source: NaCl, resulting in Cl_2 gas rather than O_2 gas (due to slow O_2 evolution kinetics [3]), Na_2SO_4, resulting in O_2 gas; however, both cells produced H_2 gas during electrolysis.

The reactions occurring at each respective electrode of the H_2/Cl_2 cell, when operating as a fuel cell, are represented in equations 3 and 4:

Anode

$$H_{2(g)} + 2OH^-_{(aq)} \rightarrow 2H_2O_{(aq)} + 2e^- \qquad (3)$$

Cathode

$$Cl_{2(g)} + 2e^- \rightarrow 2Cl^-_{(aq)} \qquad (4)$$

Similar to the H_2/Cl_2 fuel cell, the H_2/O_2 cell's anode reaction is given by equation 3, while the cathode is given by equation 6.

Cathode

$$O_{2(g)} + 2H_2O_{(aq)} + 4e^- \rightarrow 4OH^-_{(aq)} \qquad (6)$$

Using equation 2, the theoretical cell potentials were calculated, using standard reduction and oxidation potentials, (see appendix) to be 2.18 V and 2.06 V for the hydrogen-chlorine and hydrogen-oxygen fuel cells, respectively.

Experimental

Materials

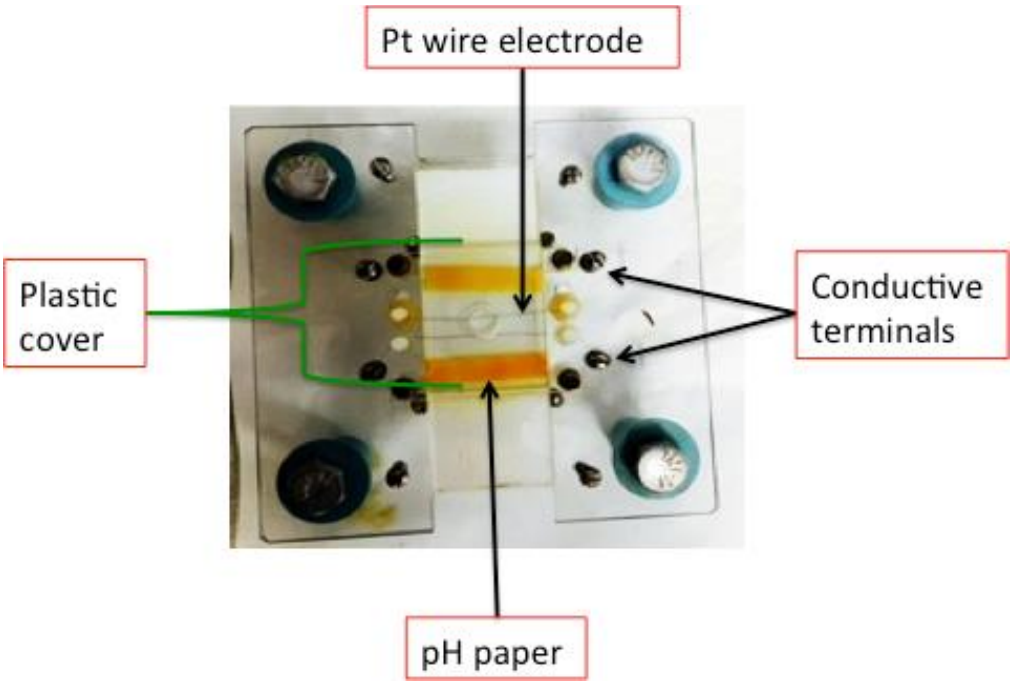

Figure 1. Thin-layer fuel cell setup used for both NaCl and Na_2SO_4 experiments. Electrolyte solution, pH paper, and Pt wires are compressed between glass microscope slide and polystyrene slide. Slides are pressed together with plastic cover screwed in to apply equal pressure across the cell.

Each fuel cell was constructed as shown in Figure 1. The fuel cell slides were cleaned using copious amounts of DI water and dried. Two Pt wires, with diameters of 0.217 mm, were placed parallel to each other across the cell and connected to two nickel-coated conductive terminals. Two strips of pH paper were cut to the width of the slide and placed to the sides of both Pt wires in order to visualize changes in pH during operation. Electrolyte solution (0.3327 ± .0003 M NaCl or 0.06689 ± .00007 M Na_2SO_4) was carefully pipetted to the cell area (while also wetting the pH paper), but it was made sure that no solution spilled out the side. A

polystyrene slide was carefully placed on top of the glass slide (making sure not to apply much pressure) and a plastic cover plate was screwed-in directly over the Pt wires and pH paper.

Voltage and current measurements

Voltage and current measurements were made by connecting the fuel cell's conductive electrodes in parallel with two multimeters (represented in Figure 2), one operating as a voltmeter and the other as a ammeter. The multimeters were each connected to individual computers to record the current and voltage in real-time. The data was saved and exported after each experiment.

Electrolysis

Before conducting any measurements, the cell was first run as an electrolyzer to produce H_2 and Cl_2 (or O_2) gas bubbles for fuel cell operation. A small photovoltaic panel was connected to the conductive electrodes of the fuel cell and a lamp was shone on the panel to apply about a ~3 V voltage. The evolution of gas bubbles at the wires was visible and the pH paper began to turn red at the anode, indicating the acidification due to partial hydrolysis (see appendix) and the production of H^+. Conversely, the cathode region turned blue, from the increased alkalinity due to the reduction of H^+. A schematic of the H_2/Cl_2 fuel cell in eletrolyzer mode is represented in Fig. 2A:

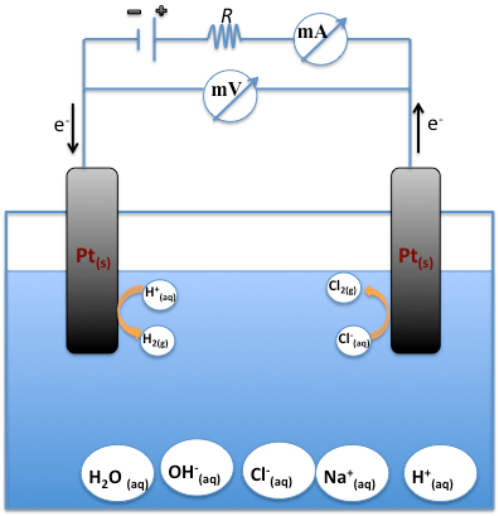

Figure 2A. Schematic diagram of H_2/Cl_2 URFC operating in eletrolyzer mode.

Fuel Cell

Performance of each fuel cell was studied by placing an external resistance load on the circuit in a descending then ascending order. The external resistances consisted of two different sets: 909-200 kΩ and 150-10 kΩ. The cells were also used to power a small 1.5 V portable calculator and a small light emitting diode (LED), measuring the cell's ability to power each device. The cell was recharged by electrolysis between external resistance sets. A schematic of the H_2/Cl_2 fuel cell in fuel cell mode is represented in Fig. 2B:

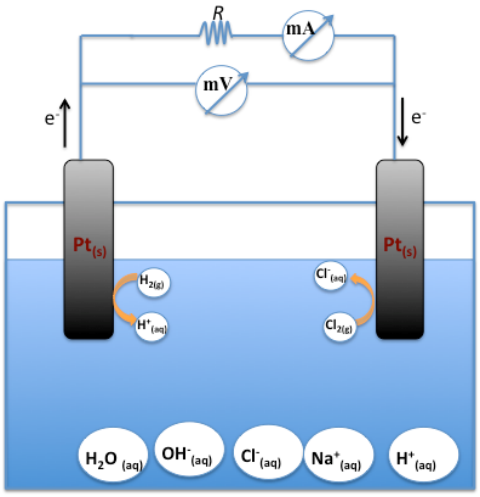

Figure 2B. Schematic diagram of H_2/Cl_2 URFC operating in fuel cell mode.

Results

The voltage and current readings of the H_2/Cl_2 and $H2/O_2$ fuel cells from the external resistor sets (both large and small) are shown in Tables 1 and 2, respectively. As the resistance decrease, the voltage also decreases, while the current density increases. The power density of the cell increased as current density increased until max power was reached, followed by decreasing power density as current density increased.

Table 1. Average voltage and current readings using large and small resistor sets for the hydrogen-chlorine fuel cell. The current density and power density were calculated using voltage and current readings (see appendix for calculations).

Resistance (kΩ)	Average Voltage (V)	Average Current (A)	Current Density (A m^{-2})	Power Density (W m^{-2})
909	2.096	2.34E-06	0.13729	0.2877
715	2.069	2.83E-06	0.16615	0.3437
604	2.056	3.42E-06	0.20075	0.4127
402	2.037	5.09E-06	0.29898	0.6091
304	2.027	6.05E-06	0.35521	0.7201
200	1.992	8.92E-06	0.52339	1.0424
200	1.983	9.07E-06	0.53249	1.0557
304	1.996	6.67E-06	0.39165	0.7818
402	2.002	5.01E-06	0.29417	0.5889
604	2.011	3.36E-06	0.19699	0.3962
715	2.012	2.84E-06	0.16647	0.3349
909	2.014	2.25E-06	0.13218	0.2662
150	2.061	1.39E-05	0.81524	1.6806
100	2.025	2.03E-05	1.19034	2.4104
80.6	1.998	2.50E-05	1.46538	2.9285
71.5	1.980	2.76E-05	1.62239	3.2121
20	1.615	7.68E-05	4.50704	7.2782
10	0.813	7.85E-05	4.60666	3.7430
10	0.683	7.99E-05	4.69178	3.2055
20	1.451	7.38E-05	4.32805	6.2818
71.5	1.943	2.53E-05	1.48327	2.8823
80.6	1.945	2.44E-05	1.42948	2.7810
100	1.959	1.96E-05	1.15184	2.2562
150	1.987	1.30E-05	0.76115	1.5121

Table 2. Average voltage and current readings using large and small resistor sets for the hydrogen-oxygen fuel cell. The current density and power density were calculated using voltage and current readings (see appendix for calculations).

Resistance (kΩ)	Average voltage (V)	Average current (A)	Current Density (A m^{-2})	Power Density (W m^{-2})
909	1.5317	1.72E-06	0.1012	0.1550
715	1.2999	1.85E-06	0.1085	0.1410
604	1.1659	1.96E-06	0.1151	0.1342
402	1.0583	2.66E-06	0.1563	0.1655
304	0.9139	3.11E-06	0.1828	0.1670
200	0.8026	3.67E-06	0.2154	0.1728
200	0.7286	3.67E-06	0.2154	0.1569
304	0.7447	2.50E-06	0.1466	0.1092
402	0.7436	1.88E-06	0.1102	0.0820
604	0.7463	1.26E-06	0.0742	0.0554
715	0.7030	1.01E-06	0.0591	0.0416
909	0.6910	7.76E-07	0.0456	0.0315
150	1.3970	9.28E-06	0.5446	0.7607
100	1.1422	1.14E-05	0.6705	0.7659
80.6	1.0807	1.23E-05	0.7240	0.7825
71.5	1.0536	1.29E-05	0.7590	0.7997
20	0.5416	2.54E-05	1.4919	0.8080
10	0.2723	2.76E-05	1.6194	0.4410
10	0.2520	1.97E-05	1.1553	0.2912
20	0.5453	1.93E-05	1.1305	0.6164
71.5	0.8137	1.10E-05	0.6434	0.5235
80.6	0.8342	9.13E-06	0.5359	0.4470
100	0.8367	7.29E-06	0.4279	0.3580
150	0.8435	5.73E-06	0.3363	0.2836

In the case of the external resistor sets, the relationship between current density and cell potential can be compared in a polarization curve; the large and small external load sets of the hydrogen-chlorine fuel cell represented in Figure 3A and 4A, respectively. While the large and small external load sets of the hydrogen-oxygen fuel cell is represented in Figure 3B and 4B, respectively.

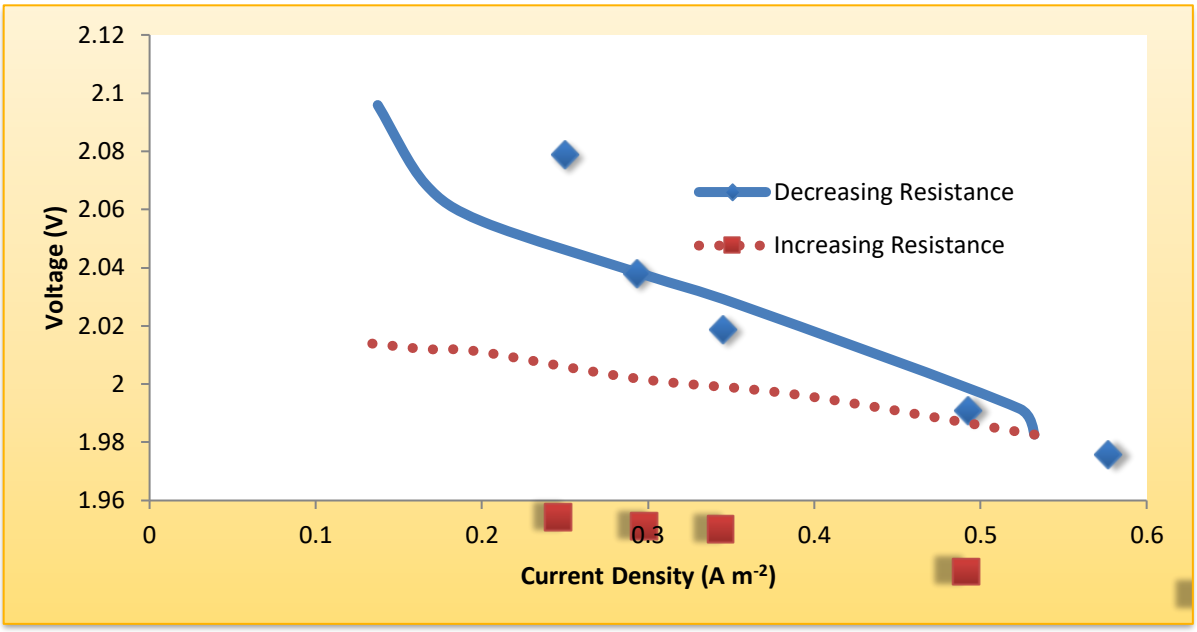

Figure 3A. Hydrogen-chlorine fuel cell, large external load set cell potential (909-200 kΩ).

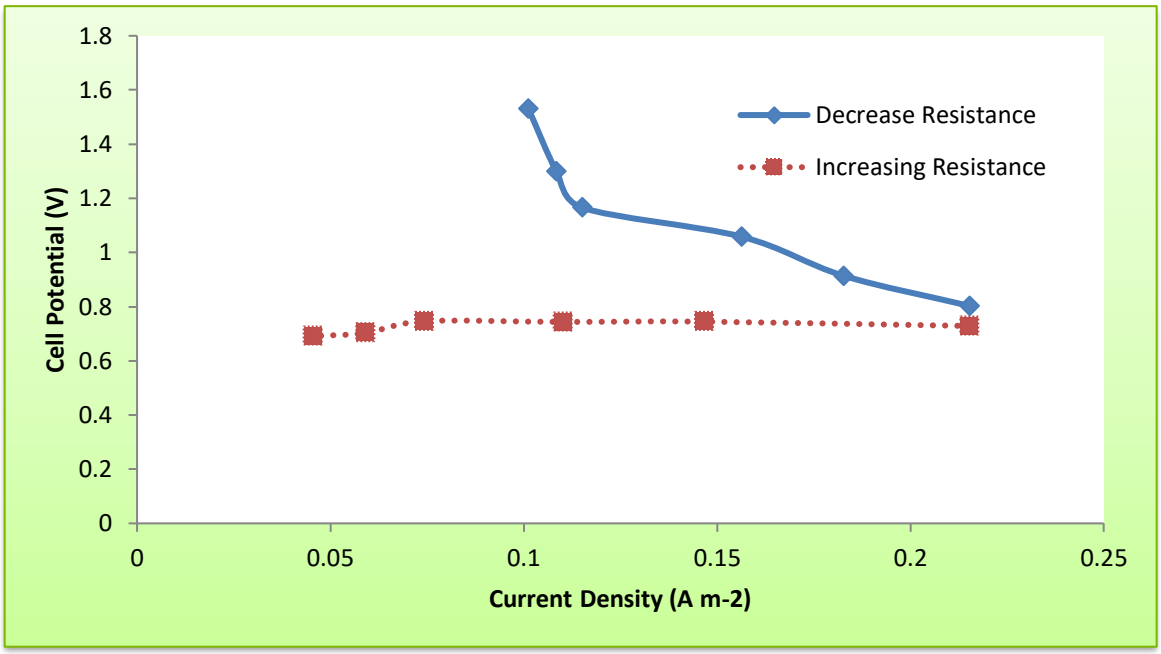

Figure 3B. Hydrogen-oxygen fuel cell, large external load set cell potential(909-200 kΩ).

The graphs of Figures 3A and B represent the linear decrease in cell potential with increasing current density. The use of "current density" rather than simply "current" takes the dimensions of the cell's electrodes into account.

At smaller external loads, the cells show similar linear trends, until there is a sharp loss of cell potential at the highest current densities (Figures 3A and B, H_2/Cl_2 and H_2/O_2, respectively).

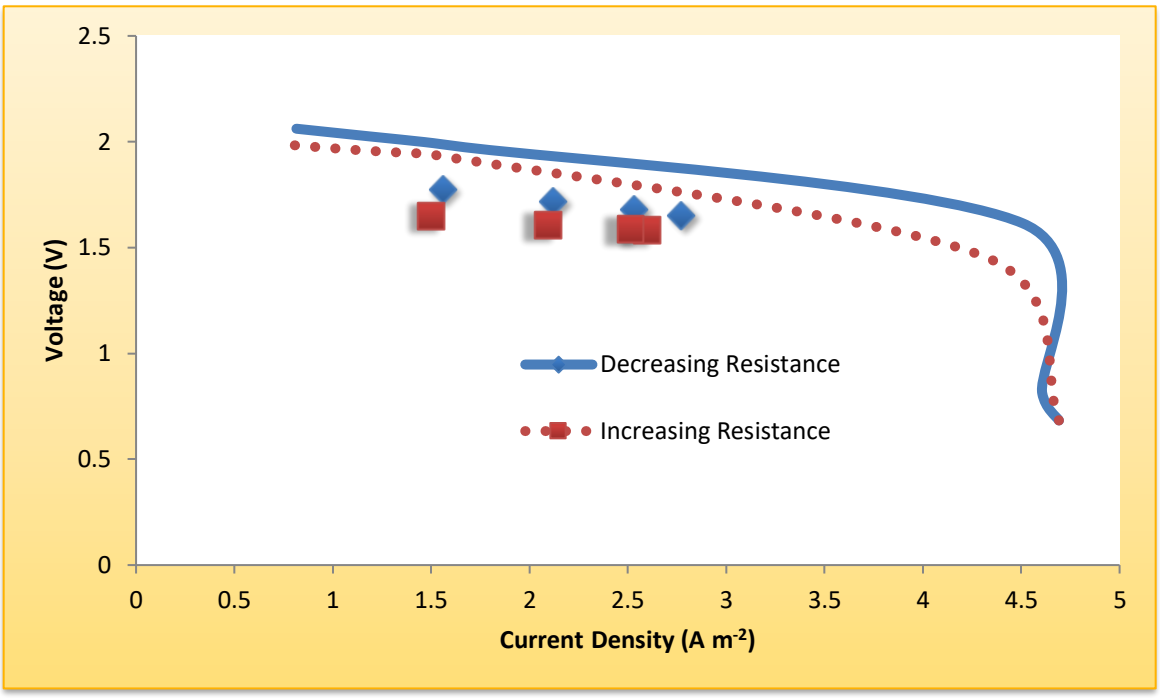

Figure 4A. Hydrogen-chlorine fuel cell, small external load set cell potential (150-10 kΩ).

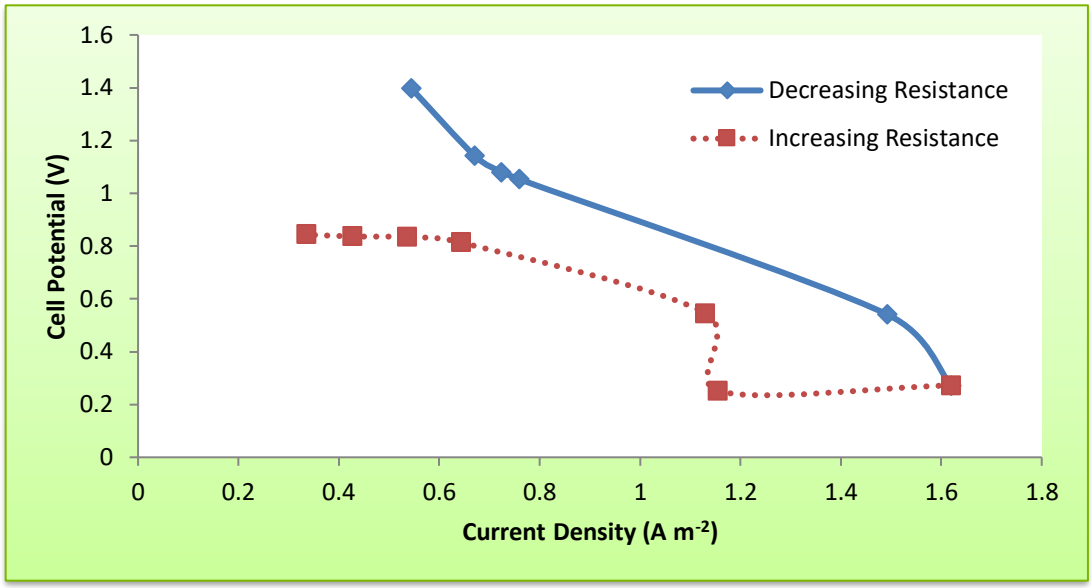

Figure 4B. *Hydrogen-oxygen fuel cell small external load set cell potential (150-10 kΩ).*

By graphing the power density as a function of current density, the linear increase in power and eventual max power can be seen. The linear increase in power for the large external load set is represented in Figure 5A and B.

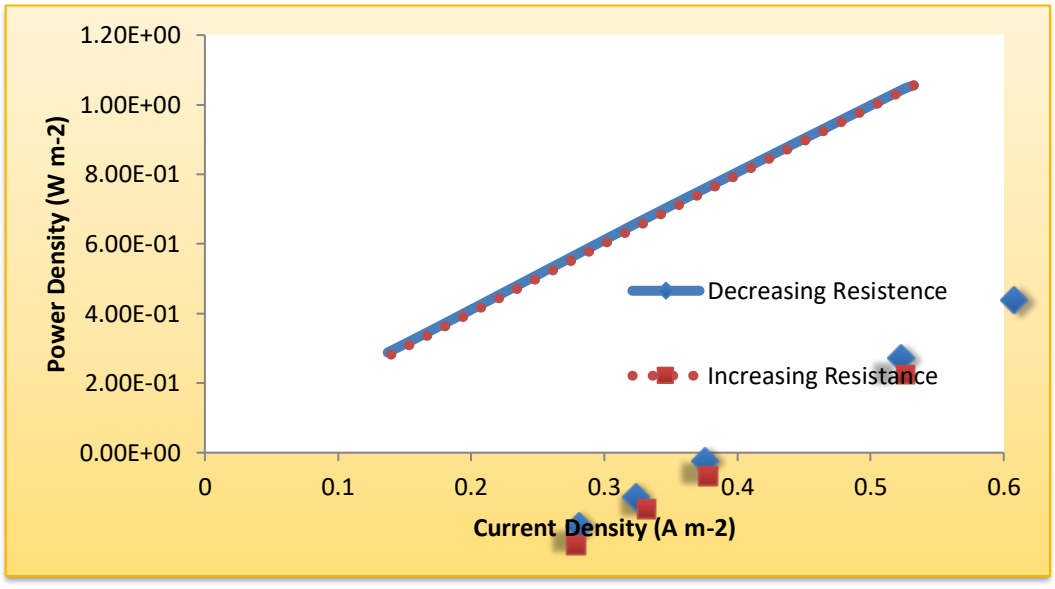

Figure 5A. *Hydrogen-chlorine fuel cell large external load set power density (909-200 kΩ).*

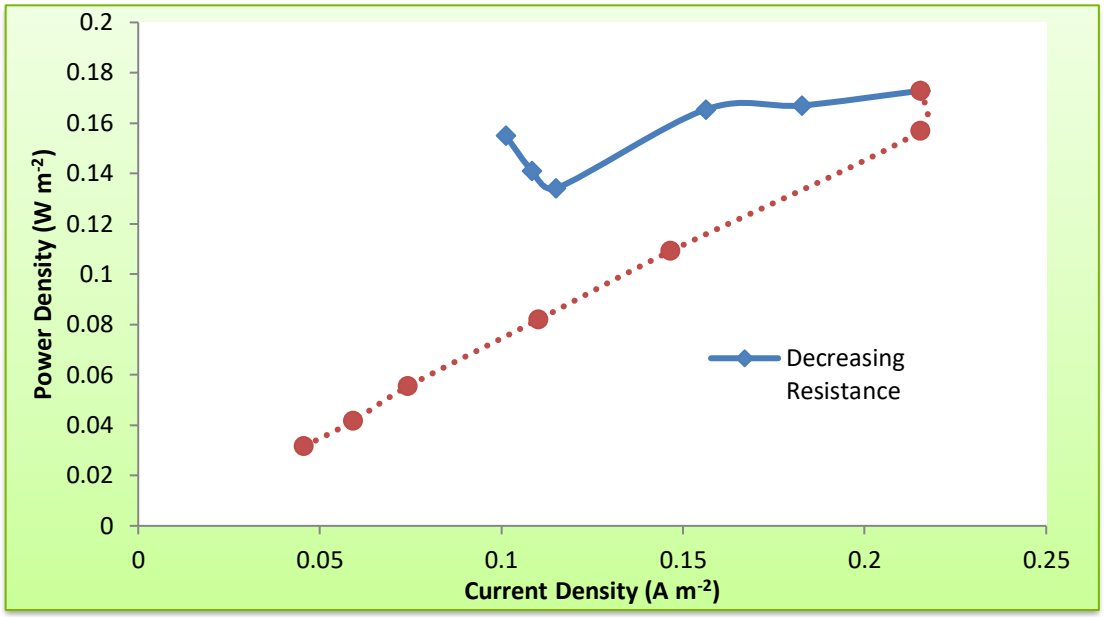

Figure 5B. *Hydrogen-oxygen fuel cell large external load set power density (909-200 kΩ).*

When the cells were switched to lower external loads, represented in Figure 6A and B, the power density maintained its linear increase, until a peak was reached and the power declined with higher current.

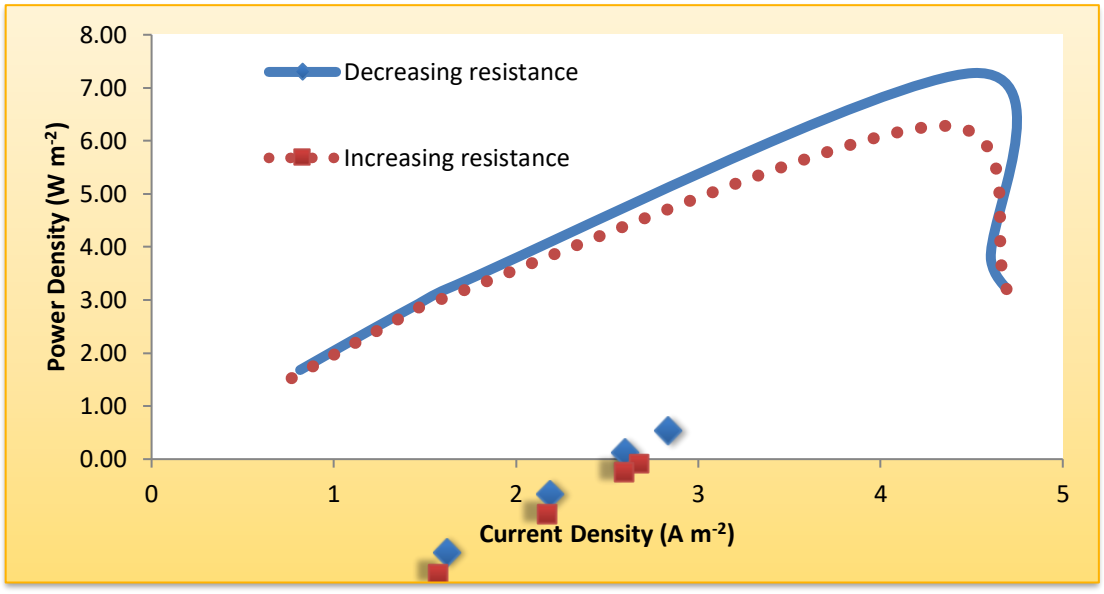

Figure 6A. *Hydrogen-chlorine fuel cell small external load set power density (150-10 kΩ).*

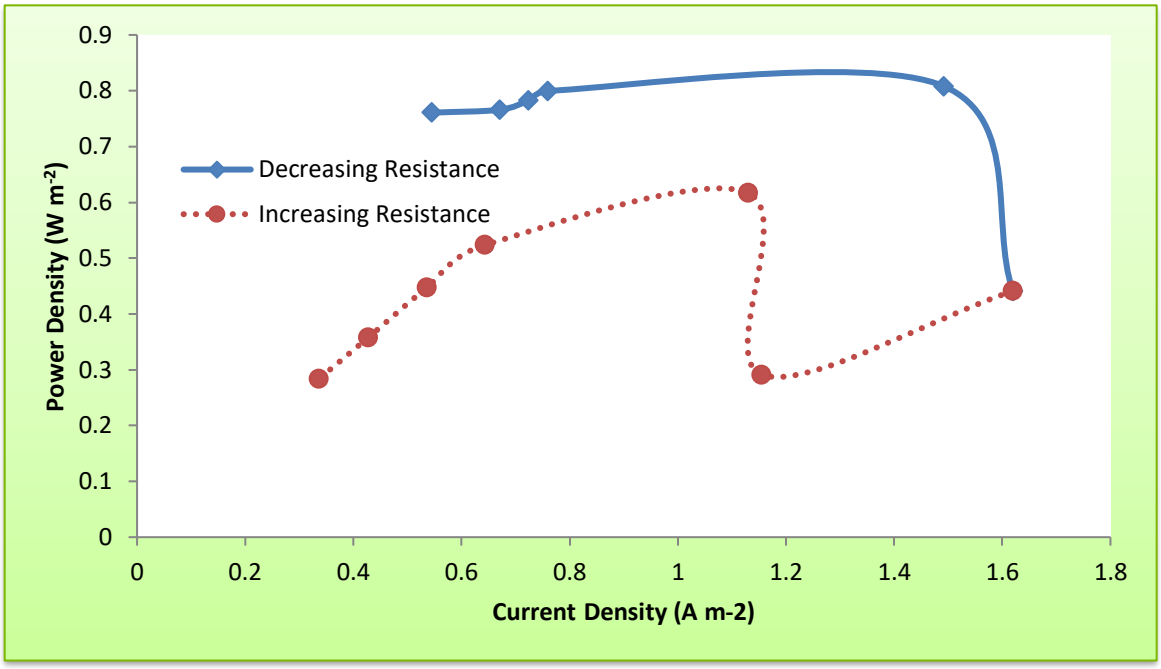

Figure 6B. *Hydrogen-oxygen fuel cell small external load set power density (150-10 kΩ).*

A polarization curve can be represented by using both data sets of external load to graph cell potential as a function of current density as the resistance decreases from 909 kΩ to10 kΩ, then increases back to 909 kΩ. The polarization curve of the hydrogen-chlorine and hydrogen-oxygen fuel cells are represented in Figure 7A and B respectively.

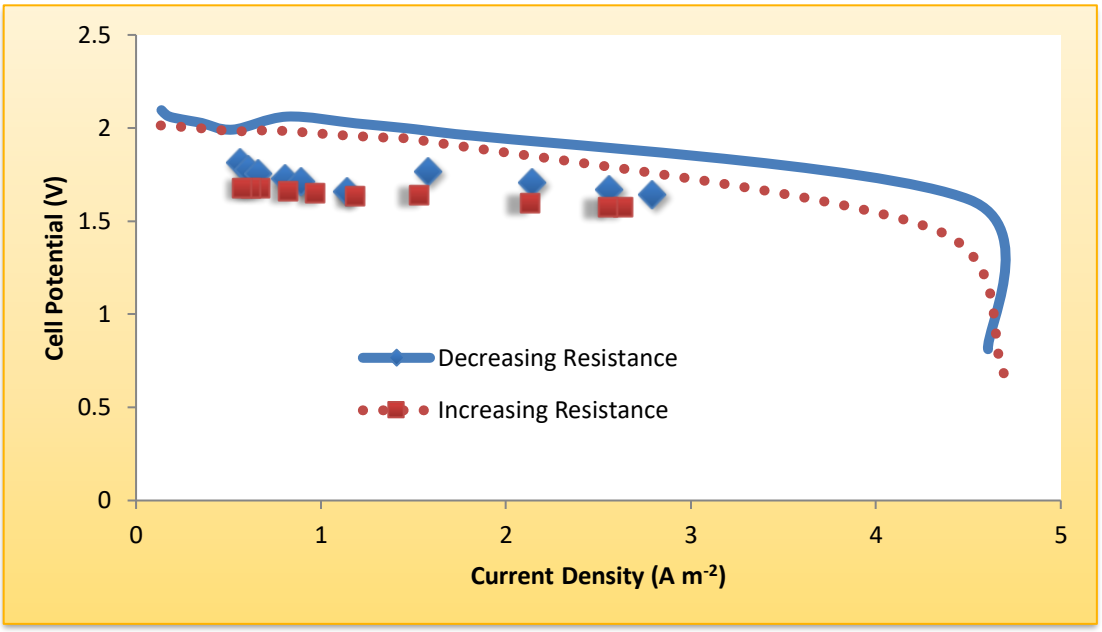

Figure 7A. Polarization curve of decreasing resistance, followed by increasing resistance for the hydrogen-chlorine fuel cell.

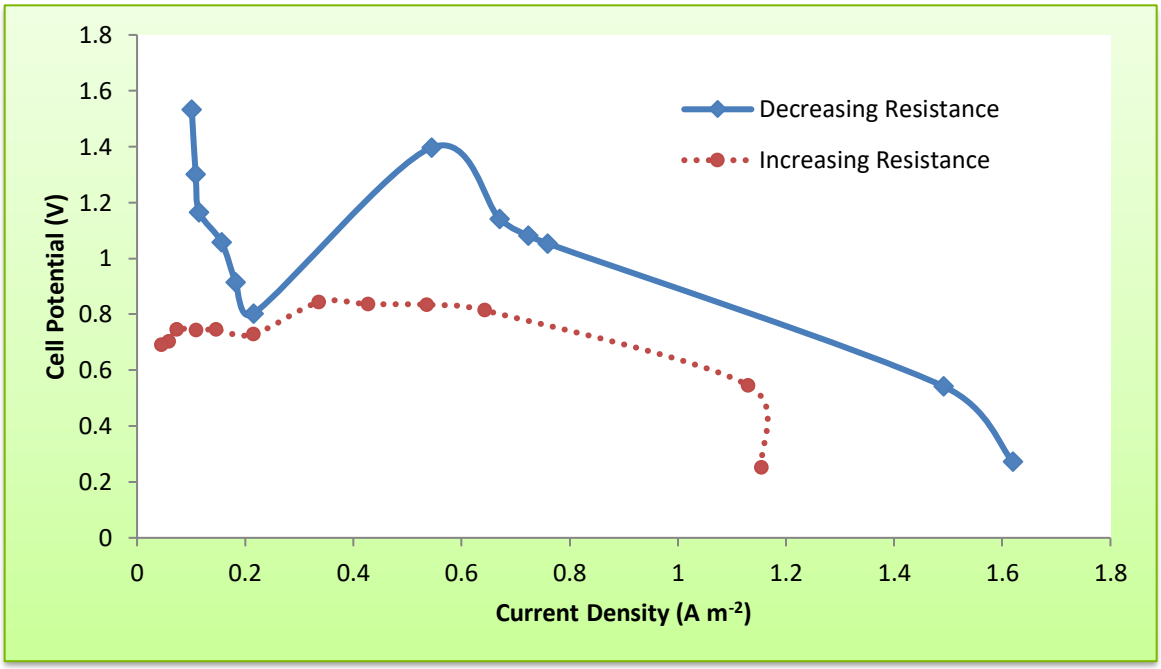

Figure 7B. Polarization curve of decreasing to increasing resistance for the hydrogen-oxygen fuel cell.

The regenerative performance of the fuel cell was also tested by using them to power a calculator (normally power by a 1.5 V battery) and a small LED. The current and voltage of the

hydrogen-chlorine fuel cell as a function of time, for powering both the LED and calculator, are shown in Figures 8A and B, respectively. The cell provided power the LED for a longer period of time, but the current decay exponential over time, while the calculator received a relatively steady supply of current. The similar current and voltage results of the hydrogen-oxygen fuel cell as a function of time, are shown in Figures 9A and 9B, respectively

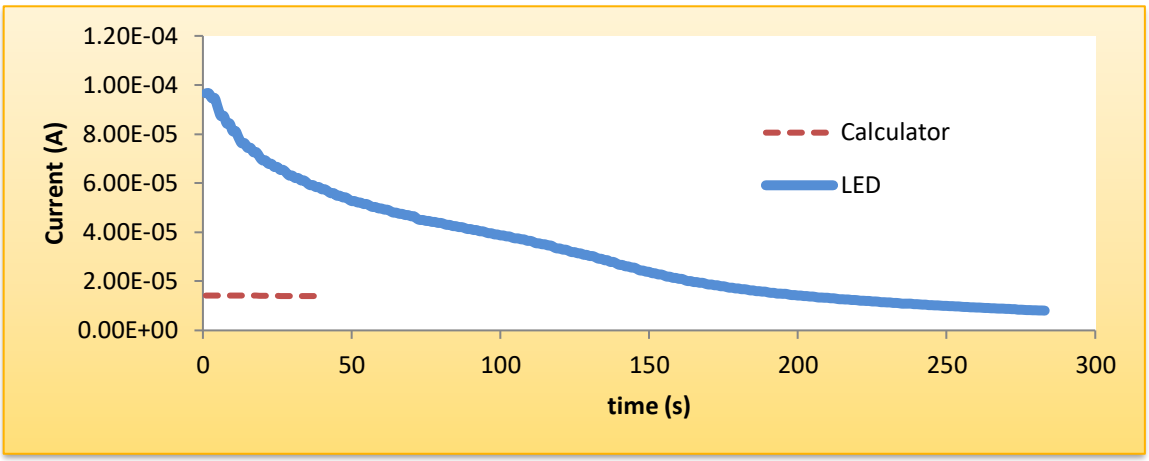

Figure 8A. *Current while powering a calculator or LED as a function of time for the hydrogen-chlorine fuel cell.*

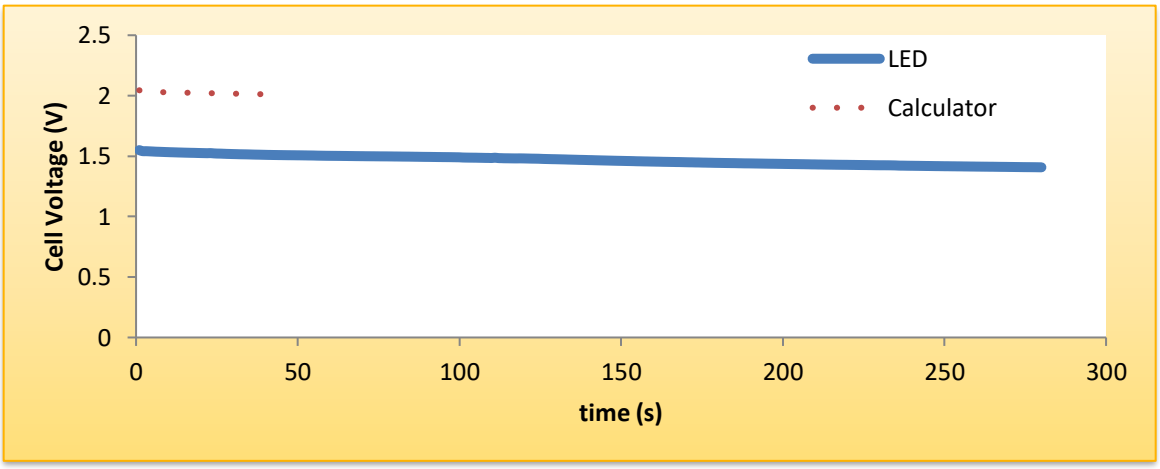

Figure 8B. *Cell potential while powering a calculator or LED as a function of time for the hydrogen-chlorine fuel cell.*

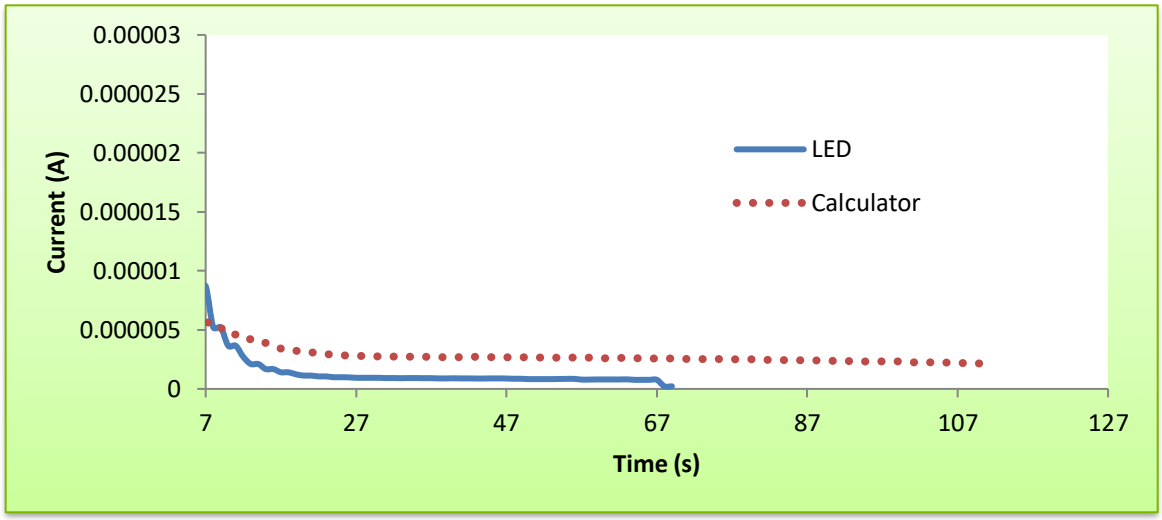

Figure 9A. Current while powering a calculator or LED as a function of time for the hydrogen-oxygen fuel cell.

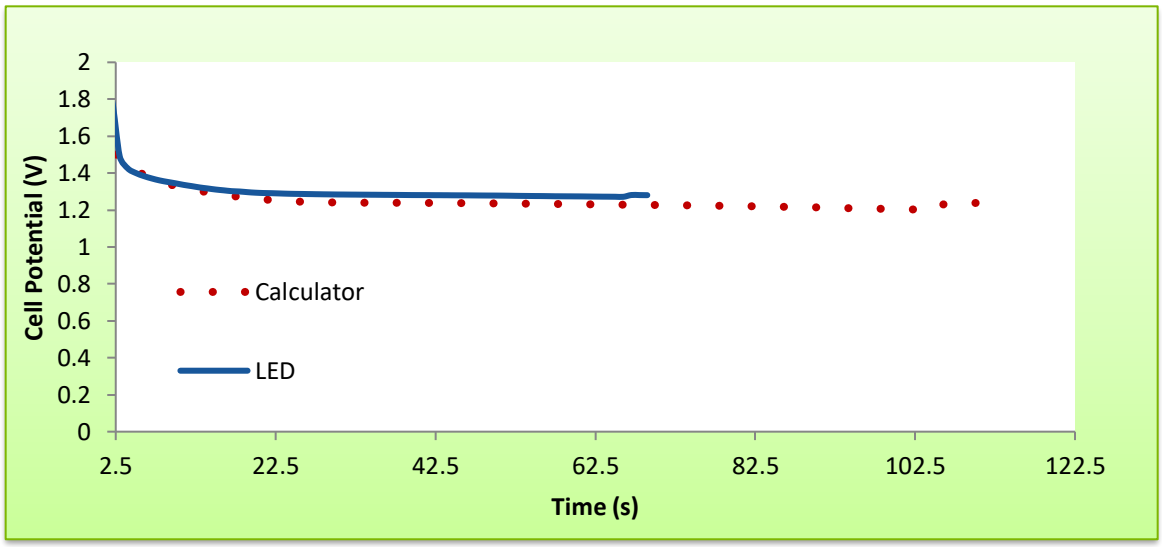

Figure 9B. Cell Potential while powering a calculator or LED as a function of time for the hydrogen-oxygen fuel cell.

Discussion

Fuel Cell Operation

The use of resistor sets (steadily increasing then decreasing external resistance) for the fuel cells reveals the linear relationship between current density and cell potential, until the mass transfer limit is reached. The small amount of current drawn from the cell during measurements

did not significantly affected the cell's activity [3], exhibited by the small magnitude of hysteresis in the reverse direction (increasing resistance) of the H_2/Cl_2 fuel cell; these effects are more prevalent in the polarization curve shown in Figure 7A. The cause of the mass transport, seen in Figures 7A, can be attributed to the slow rate of hydrogen dissolution, which causes the dissolved hydrogen of the system near the anode to be depleted [3].

When operating the H_2/O_2 fuel cell the magnitude of hysteresis was much larger (Figure 7B), caused by a large current being drawn from the cell's lower potential during measurements (compared to the H_2/Cl_2 fuel cell). This non-ohmic behavior may be due to the lower open cell potential of the hydrogen-oxygen cell (compared to hydrogen-chlorine) and the lower concentration [3] of electrolyte used to make the hydrogen-oxygen cell (0.06689 M Na_2SO_4 compared to 0.333 M NaCl). The mass-transport effect also appears in the polarization curve of the H_2/O_2 cell (Figure 7B).

The power density of the fuel cell was also in agreement with the polarization curve's mass transport, as Figures 5A and 5B shows a linear increase in power with current. The continuation of this trend can be seen in Figures 6A and B until a maximum power of 7.28 W m^{-2} for the H_2/Cl_2 cell and 0.81 W m^{-2} for the H_2/O_2 cell is reached, followed by a decrease in power density with further increased current density. As expected, the H_2/O_2 fuel cell exhibited lower power compared to the H_2/Cl_2 cell, due to the hydrogen-oxygen cell's lower open cell potential and oxygen's lower solubility (compared to chlorine) [4].

Regenerative Fuel Cell Performance (Calculator and LED)

To As shown in Figures 8A and B, the hydrogen-chlorine fuel cell maintained a steady cell potential while powering both devices. The calculator maintained a steady current and voltage throughout its run, while the powering of the LED caused a surge in current, followed by

an exponential decay, providing power for ~5 minutes. Similar to the hydrogen-chlorine cell, the hydrogen-oxygen cell maintained a steady cell potential when powering both devices (Figure 9A); however, the current decayed much faster (due to the lower potential of H_2/O_2), providing power to the LED for a little more than 1 minute (Figure 9B). The realistic application of the fuel cell, in order to power a calculator and LED, demonstrates the potential of these cells to be used as clean and reliable energy sources.

The pH gradient along the thin-film of the cell causes the larger rest potential observed during the experiment. As the pH gradient slowly moves towards equilibrium, the rest potential of the cell also decreases; however, the thin-layer design of this fuel cell stabilizes the pH gradient near the electrode and allows for the rest potential to remain stable for a longer period of time.

Conclusion

The performance of both H_2/Cl_2 and H_2/O_2 thin-layer fuel cells were studied by applying an external resistance to the circuit. The design of the fuel cells allowed for efficient regeneration of the fuel cell by electrolysis. The H_2/Cl_2 fuel cell exhibited a greater open cell potential of ~2.10 V compared to the ~1.20 V of the H_2/O_2 fuel cell. The H_2/Cl_2 fuel cell provided a greater maximum power ~7.28 W m^{-2} compared to ~0.81 W m^{-2} of the H_2/O_2 fuel cell, due to the higher OCP of the H_2/Cl_2 fuel cell and the lower solubility of oxygen. Both cells were capable of powering the calculator and LED, although the hydrogen-chlorine cell powered the LED for ~4 minutes longer than the hydrogen-oxygen cell. These results demonstrate the greater efficiency of the H_2/Cl_2 unitized regenerative fuel cell and its potential as a small, effective, and clean energy source.

References

1. Koh, Shirlaine, and Peter Strasser. "Electrocatalysis on bimetallic surfaces: modifying catalytic reactivity for oxygen reduction by voltammetric surface dealloying." *Journal of the American Chemical Society* 129, no. 42 (2007): 12624-12625.
2. Atkins, P. W. "Physical Chemistry. 6th." (1998).
3. "Thin-Layer Fuel Cell for Teaching and Classroom Demonstrations." *Journal of Chemical Education* 86, no. 3 (2009): 324.
4. Joe, JM Chin Kwie, L. J. J. Janssen, S. J. D. Van Strelen, J. H. G. Verbunt, and W. M. Sluyter. "Bubble parameters and efficiency of gas bubble evolution for a chlorine-, a hydrogen-and an oxygen-evolving wire electrode." *Electrochimica Acta* 33, no. 6 (1988): 769-779.

Sample Calculations

Concentration of sodium chloride

$$c = \frac{m_{NaCl}}{\left(MW_{NaCl}\right) * \left(V_{solvent}\right)} = \frac{1.944 g}{\left(58.44 \frac{\text{g}}{\text{mol}}\right) * \left(0.100 \text{L}\right)} = 0.3327 \text{ M}$$

Where *MW* is the molecular weight, *m* is the mass used, and *V* is the volume.

Partial hydrolysis half reactions of the H_2/Cl_2 cell

$$Cl_{2(g)} + H_2O_{(aq)} \rightarrow HClO_{(aq)} + Cl^-_{(aq)} + H^+_{(aq)}$$

$$HClO_{(aq)} \rightarrow ClO^-_{(aq)} + H^+_{(aq)}$$

Theoretical cell potential of H_2/Cl_2 cell

$$E^\circ_{cell} = \text{oxidation potential + reduction potential}$$

$$E^\circ_{cell} = 1.39 \text{ V} + 0.83 \text{ V} = 2.18 \text{ V}$$

Theoretical cell potential of H_2/O_2 cell

$$E^\circ_{cell} = \text{oxidation potential + reduction potential}$$

$$E^\circ_{cell} = 1.23 \text{ V} + 0.83 \text{ V} = 2.06 \text{ V}$$

Total electrode area

$$A = (r * p) * (l) * 2 \text{ wires}$$
$$= (0.0001085 \text{ m}) * p * (0.025 \text{ m}) * 2 = 0.00001704314 \text{ m}^2$$
$$= 1.704 * 10^{-5} \text{ m}^2$$

Current density for 909 kΩ resistance of H_2/Cl_2 cell

$$J = \frac{I}{A} = \frac{2.3394 * 10^{-6} A}{1.704 * 10^{-5} \text{ m}^2} = 0.1373 \text{ A m}^{-2}$$

Power density for 909 kΩ resistance of H_2/Cl_2 cell

$$P = JV = (0.1373 \text{ A m}^{-2}) * (2.0959 \text{ V}) = 0.2877 \text{ W m}^{-2}$$

Error Calculations

Uncertainty in stock concentration of NaCl

$$Dc = \sqrt{\left(\frac{\partial c^2}{dm^2}\right) * (dm^2) + \left(\frac{\partial c^2}{\partial V^2}\right) * (dV^2)} = 0.0003 \text{ M}$$

Raw Data

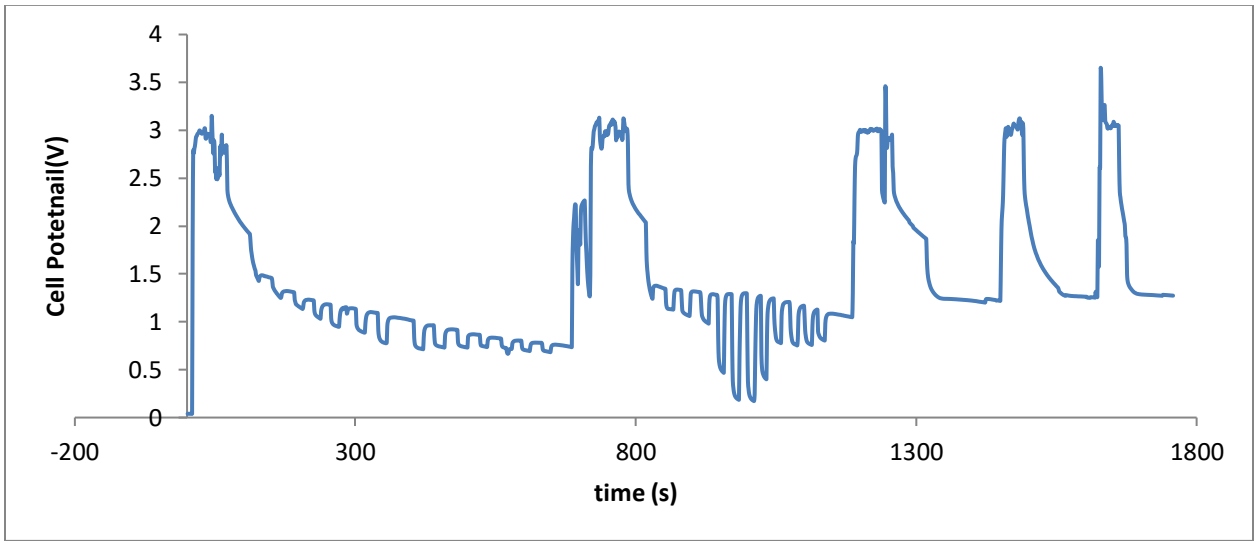

Figure A1. *Cell Potential as a function of time for all measurements of the hydrogen-oxygen fuel cell.*

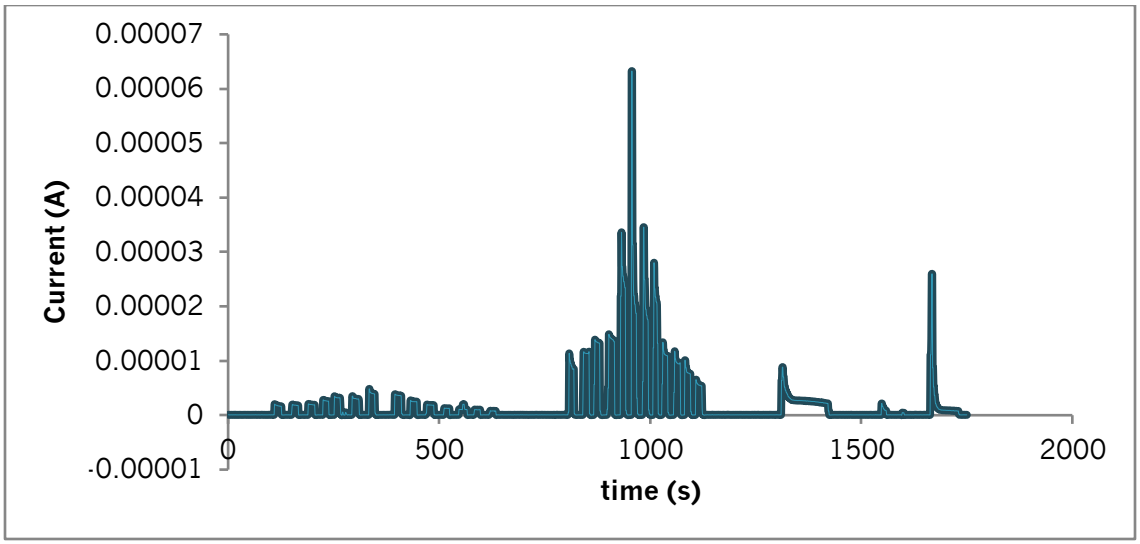

Figure A2. *Current as a function of time for all measurements of the hydrogen-oxygen fuel cell.*

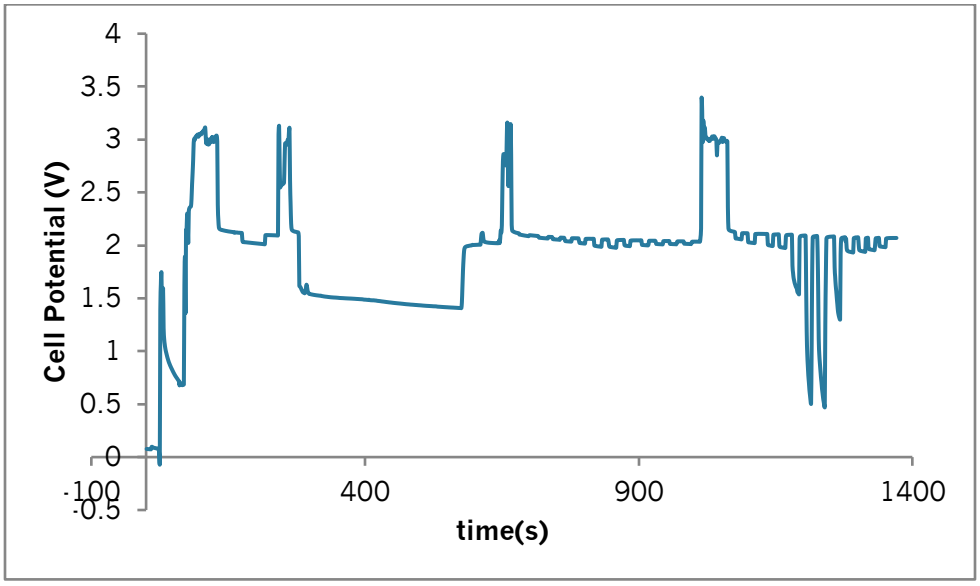

Figure A3. *Cell potential as a function of time for all measurements of the hydrogen-chlorine fuel cell.*

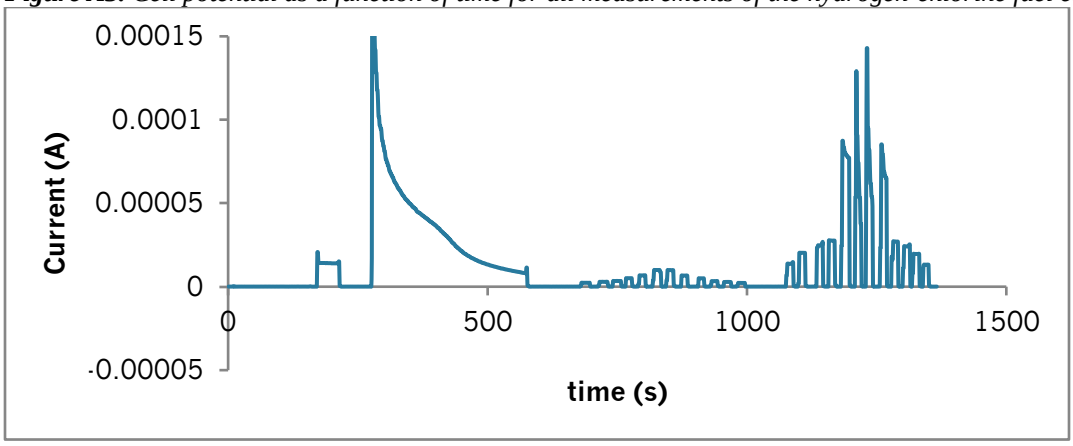

Figure A4. *Current as a function of time for all measurements of the hydrogen-chlorine fuel cell.*